ScieRxiv
NOT PEER-REVIEWED
Original Article

Immune modulation in ER+/PR+ breast cancer by extracellular vesicle–mediated hsa-miR-27a-3p through the PD-L1/PD-1 axis

Abdulwahab Teflischi Gharavi[1,2], Raheleh Tahmasvand[1], Razieh Dalirfardouei[3], Amirabbas Rahimi[4], Morteza Karimipoor[4], Saeed Irian[2], Asadollah Mousavi[5], Azadeh Niknejad[2], Mona Salimi[1]*, Ana Claudia Torrecilhas[6]*

[1]Department of Physiology and Pharmacology, Pasteur Institute of Iran, Tehran 1316943551, Iran.
[2]Department of Cell and Molecular Sciences, Faculty of Biological Sciences, Kharazmi University, Tehran 1571914911, Iran.
[3]Research center for Molecular Medicine, Hamadan University of Medical Sciences, Hamadan 6516717673, Iran.
[4]Molecular Medicine Department, Biotechnology Research Center, Pasteur Institute of Iran, Tehran 1316943551, Iran.
[5]Hematology, Oncology and Stem Cell Transplantation Research Center, Tehran University of Medical Sciences, Tehran 1416753955, Iran.
[6]Departamento de Ciências Farmacêuticas, Diadema Campus, Instituto de Ciências Ambientais, Químicas e Farmacêuticas, Universidade Federal de São Paulo (UNIFESP), Diadema, São Paulo 09972270, Brazil.

***Correspondence to:** Dr. Mona Salimi, Department of Physiology and Pharmacology, Pasteur Institute of Iran, Tehran 1316943551, Iran. E-mail: salimimona@pasteur.ac.ir; Dr. Ana Claudia Torrecilhas, Departamento de Ciências Farmacêuticas, Diadema Campus, Instituto de Ciências Ambientais, Químicas e Farmacêuticas, Universidade

Federal de São Paulo (UNIFESP), Diadema, São Paulo 09972270, Brazil. Email: ana.torrecilhas@unifesp.br

Received: 12 June 2026 | Approved: 25 June 2026 | Online: 25 June 2026

Abstract

Aim: Tumor immune microenvironment (TIME) components provide two functions in breast tumors: they either inhibit tumor progression or promote tumor growth. Breast cancer cells produce microRNA (miRNA)-rich extracellular vesicles (EVs), which promote tumor growth by regulating the immune response. Herein, our study aims to find how EVs derived from MCF-7 cells cause an imbalance in the immune system.

Methods: In this study MCF-7-derived EVs were isolated using size exclusion chromatography column (IZON), and then characterized by DLS, TEM, flow cytometry and Western blotting analysis. Following incubating the EVs with ER+/PR+ breast cancer patients PBMCs, the uptake of the PKH26 labeled-EVs was evaluated using confocal microscopy and flow cytometry. Immunomodulatory effects of EVs were assessed by employing ELISA method, flow cytometry, and qRT-PCR. A microRNA and gene target were discovered and validated using bioinformatic analysis and qRT-PCR.

Results: Our findings revealed an elevation of PD-L1 level in the monocyte subpopulation of ER+/PR+ breast cancer patients PBMCs following EVs phagocytosis, which led to an enhanced activity of Th2 and Tregs and reduced quantity of IFN-γ . We also identified and verified the EVs miR-27a-3p, the agent responsible for targeting and negatively regulating PTEN.

Conclusion: Overall, we suggested that EVs-derived hsa-miR-27a-3p might act through PD-L1/PD-1 axis leading to a skew in Th1, Th2 and Tregs distribution as well as modulates PTEN. Our findings can potentially guide the future development of novel theranostic targets for breast cancer.

Keywords: Breast cancer, extracellular vesicles, immune system, miRNA, PBMCs, TIME

INTRODUCTION

Immunological components present in tumor microenvironment, known as tumor immune microenvironment (TIME), are involved in numerous cancer-related processes including tumor suppression, tumor progression and metastasis[1]. TIME has been recognized as a network interaction between tumor cells and immunological agents, such as lymphocytes like T and B cells, neutrophils, natural killers (NKs), dendritic cells (DCs) and macrophages along with their subtypes and/or non-cellular components including tumor-derived chemokines, humoral factors and diverse types of cytokines[2]. Fundamentally, TIME components have dual functions in breast tumors where they act against tumor progression or have a tumor promoting role[3]. In particular, $CD8^+$ cytotoxic T cells, $CD4^+$ T helper1 (Th1), and M1 polarized macrophages function as tumor suppressors, while myeloid derived stromal cells (MDSC), $CD4^+$ T helper 2 (Th2), T regulatory cells (Treg), and M2 polarized macrophages function as tumor promoters. (4). Besides, N2 neutrophils also trigger metastasis through the activation of inactive tumor cells.

Of note is the variation in TIME composition among different patients at different stages of tumor[5], which has prompted an extensive investigation into the nature of alteration in its composition to further enhance our comprehension of the cancer nature and provide a novel and efficient cancer treatment strategy[6,7]. In terms of breast cancer, it was shown that the interaction between cancer and immune cells provides further insight into tumor progression to find valuable prognostic factors. In this context, a skewed balance in the population of Th1, Th2 and Treg cells could be considered as a cancer prognostic indicator in breast tumors[8,9]. For ER+/PR+ breast tumors, tumor-associated lymphocytes serve as both a standalone prognostic factor and an indicator of aggressiveness, predicting overall survival[10,11].

Breast cancer cells employ numerous strategies to modify the immune system named immunoediting process[12]. The variety of factors, such as soluble molecules including cytokines, chemokines, and metabolites, ligands that influence cell-cell interaction, and/or cancer-derived EVs comprising exosomes contribute to the recruitment of pro-tumor immune cells or inactivation of immunostimulating cells in order to facilitate tumor progression[13,14]. EVs are membranous particles in the size of nano, released by various cells and enclose a broad array of biomolecules such as lipids, polysaccharides, proteins, nucleic acids like DNAs as well as non-coding RNAs like lncRNAs, circRNA and mircoRNAs (miRNAs)[15-17]. Indeed, EVs take a part in intercellular communication through transferring their contents[18]. It is worth to mention that EVs are categorized into four primary groups as outlined by the International Society of Extracellular Vesicles (ISEV), among which, exosomes are identified as small EVs (sEVs) and ranged between 30-200 nm[19,20]. Recently, there has been a notable surge in scientific research towards the tumor immune response mediated by EVs [28]. In fact, EVs can deliver tumor antigens to antigen presenting cells (APCs), thereby triggering the adaptive immune response[21]. In contrast, the EVs released by cancerous cells can modulate the immune responses to make easier the tumor progression[22].

Breast cancer cells release miRNA-rich EVs which cause tumor progression by modulating the immune response[23]. In this regard, MCF-7 derived exosomes encapsulating miRNA-222 (miR-222) can directly target PTEN and cause M2 macrophage polarization leading to tumor development[24]. Moreover, stress-induced exosomal miR-27a-3p secretion promotes MCF-7 cells immune escape through up-regulation of PD-L1 via the MAGI2/PTEN/PI3K pathway[25]. In breast cancer research, there is a clear lack of immunomodulatory studies regarding the impact of ER+/PR+ breast cancer derived EVs on the balance of Th1, Th2 and Treg cells in patients PBMCs. This motivated us to isolate EVs derived from MCF-7 cells as a model for ER/PR positive breast cancer and co-incubate them with PBMCs obtained from ER+/PR+ breast cancer patients' blood. Besides, we attempted to find a microRNA in EVs with a potential immunomodulatory role using systems biology.

METHODS

Cell culture and EV isolation

MCF-7 (C10082) cells as ER+/PR+ breast cancer cell line were purchased from the Iranian Biological Resource Center (IBRC, Iran) and utilized as a source for cancer-derived EVs. To isolate the EVs, 2.5 × 10^5 cells were transferred into 75 cm^2 cell culture flasks (SPL Life Sciences, Korea) containing DMEM, 10% FBS, and 1% pen-strep (all from Gibco, USA). Once the cell confluency reached 80%, the culture medium was replaced by DMEM with 10% exosome-free FBS (Gibco, USA) for 48 h. Afterwards, the conditioned media were collected, and the cell debris was eliminated through centrifugation at 1,500 × g for 10 min at 4 °C. To further separate out larger extracellular vesicles, the supernatant underwent centrifugation at 10,000 × g for 30 min. Subsequently, the remaining supernatant was concentrated utilizing the Amicon Stirred Cell (UFSC20001, USA) with the membrane of 100 kDa cutoff (Millipore, USA). Finally, the concentrated medium was applied onto a 70 nm qEV size exclusion column (IZON, New Zealand), and then fractions 1-3 which mainly contained EVs, were collected. The retrieved solution was concentrated using 100 kDa cut-off filters (Amicon Ultra-50) by centrifugation at 3,000 × g at 4 °C for 30 min [Figure 1].

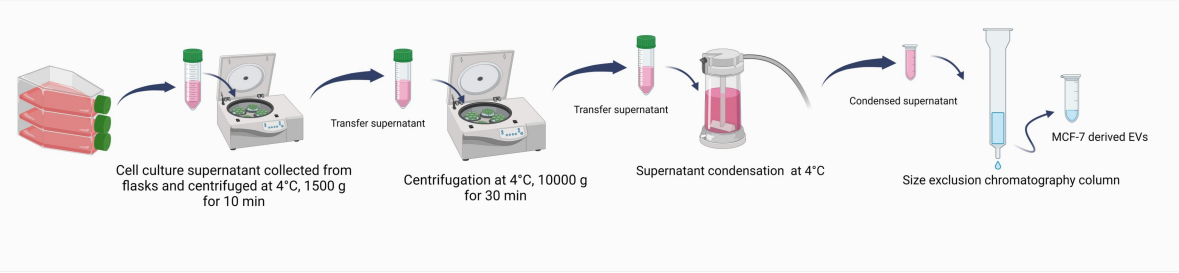

Figure 1. Flow chart of the procedure used to obtain EV-enriched fractions by size exclusion chromatography column (Izon). The supernatant of cell culture was collected and underwent a set of centrifugation steps at progressively higher spin speeds. Large particles including dead cells, cell debris, and apoptotic bodies were removed using two differential centrifugation steps (1,500 g and 10,000 g). EV-enriched supernatant was concentrated using Amicon stirred cell and applied onto a 70 nm qEV size exclusion column.

Measurement of EVs size by DLS

Size distribution of the isolated EVs was evaluated via dynamic light scattering (DLS) (Malvern Instruments Ltd. Nano-ZS). To do this, 100 µL of the concentrated EVs solution was mixed with 1 mL of PBS, passed through a 0.22 µm syringe filter (Membrane Solutions, USA), vortexed at room temperature for 15 seconds, and then transferred to the designated cuvette. Measurements were performed for the samples based on intensity and number, to assess both the size and distribution of the particle sizes at a temperature of 25 °C.

Assessment of EVs morphology by TEM

The morphology of MCF-7 isolated EVs was visualized using transmission electron microscopy (TEM). To perform this, 50 µL of the concentrated EVs suspension was mixed with 200 µL of PBS, and then fixed using 3% glutaraldehyde in a 1:1 ratio. A drop of this mixture was then placed on a grid coated with Formvar. The samples were negatively stained with 2% uranyl acetate for 2 min and air-dried for 1 h. After washing with distilled water, the dried copper grids were observed under a Zeiss EM900 transmission electron microscope at 80 kV (Germany) to analyze the size and shape of EVs.

Protein quantification

Bicinchoninic acid (BCA) protein assay (DNAbiotech, Iran) was employed to quantify protein concentration of the EVs according to the kit instruction. In summary, a small volume of each sample (25 µL) was combined with 75 µL of working reagent (50:1 ratio of assay reagents A to B), and subsequently dispensed into 200 µL microtubes. Following incubation for 1 h at 60 °C, the absorbance was measured using a spectrophotometer (BioTek, USA) at a wavelength of 562 nm.

Western blotting

MCF-7 cells and cells-derived EVs samples were lysed using DTT and RIPA lysis buffer. Following incubation on ice for 15 min and vortexing for 60 s to release the

protein content of the EVs, the samples were further incubated at 95 °C for 10 min. Total protein concentration was measured using a spectrophotometer (BioTek, USA) at a wavelength of 280 nm. Afterwards, 100 µg of protein extract was mixed by glycerol and bromophenol blue and loaded on a 12% polyacrylamide gel. The antibodies listed below were utilized: TSG 101 (ab125011, Abcam, UK), Calnexin (sc-11397, Santa Cruz, USA), β-actin (6018, Cell Signaling, USA) in 1:1,500 dilution of each and secondary horseradish peroxidase-linked antibody goat anti-rabbit (1:2,000 ratio) (15443, Cell Signaling, USA).The blots were visualized with the ECL Western blotting detection kit (Amersham, UK).

EVs surface markers analysis

The presence of three surface EVs markers such as CD9, CD63 and CD81 was evaluated using the flow cytometry technique[26]. Briefly, 100 µL of the EVs sample was mixed up with 100 µL of sterile PBS containing one of the specific antibodies against EV markers including CD9-APC (312107, Biolegend, USA), CD63-FITC (353005, Biolegend, USA) and CD81-PE (349505, Biolegend, USA) with 1:50 dilution ratio of each , and then incubated at 4 °C for 30 min. After calibration by reference bead mix, the tubes were immediately subjected to measurement by Flow cytometry e (BD FACSCalibur, USA). Notably, all data were compared to PBS as a negative control. The data acquired by flow cytometry was analyzed using FlowJo software v7.6 (FlowJo LLC, USA).

EVs labeling by PKH-26

In order to track the EVs uptake, MCF-7 cells derived EVs were labeled with the membrane intercalating dye PKH-26 (Sigma-Aldrich, USA) based on the manufacture's protocol[27]. Briefly, 150 µL of the EVs suspension was brought to 1 mL with Diluent C, followed by adding PKH26 and incubating at room temperature for 5 min. To terminate the over staining of EVs, FBS 10% in PBS was added to the mixture. Upon adding 0.971 M sucrose solution to the mixture, the sample was centrifuged at 120,000 g for 2 h at 4 °C. The EVs pellet was resuspended in PBS and transferred to an Amicon 10 kDa MWCO (Millipore, USA) filter column and spun at

3000 xg in a high-speed centrifuge for 40 min. The recovered PKH-26 labeled EVs were stored in a microfuge tube on ice.

Breast cancer patients' criteria

Based on the medical profiles of patients, women with non-metastatic ER+/PR+ breast cancer were included in our study. In this context, twelve female patients (aged 45-65) diagnosed with ER+/PR+ non-metastatic breast cancer who had received no chemotherapy or underwent no surgery were chosen for this study. The informed consent was obtained from all patients or their legal guardian(s).

Isolation of patients' PBMCs

Whole blood was collected from mentioned breast cancer patients. To isolate PBMCs, 5 mL of whole blood was mixed with 5 mL of PBS and then transferred into 15 mL tubes containing 5 mL Ficoll (Lymphodex, Inno-Train, Germany). Following centrifugation at 1,700g for 15 min, the PBMC monolayer was harvested and re-suspended in 10 mL of PBS and further centrifuged at 1,000 g for 7 min. For further purification, PBMCs pellets were washed at least 2 times by 10 mL of PBS followed by centrifugation at 480g for 10 min.

EVs internalization and confocal microscopy

To assess the uptake of EVs, 1×10^6 PBMC cells were seeded in 48 well plates (SPL Life Sciences, Korea) and incubated overnight at 37 °C. PKH26 labeled EVs were filtered by 0.22 µm syringe filter, and then added to the well plates containing RPMI media (Gibco, USA) and 10% exosome-free FBS (Gibco, USA) and incubated for 24 h in a cell incubator. Afterwards, the culture media were transferred into 1.5 mL conical tubes and centrifuged at 1,000g for 5 min. The supernatant was discarded and the PBMCs pellet was fixed using paraformaldehyde (4%) for 30 min at 4 °C. PBMC cell nuclei were stained using Hoechst 33,258, and a slide lam was prepared from them. The untreated PBMCs were considered as negative control. The outcomes were evaluated using a confocal microscope (Nikon Ti-E, Japan).

EVs uptake assay using flowcytomery

To further verify the uptake of EVs by PBMCs, PKH-26 labeled EVs were filtered, and then added to culture media containing 2 × 10^6 PBMCs. PBMCs were harvested and transferred into 1.5 mL microtubes and then the percentage of PKH-26 uptake by lymphocytes and monocytes was analyzed by flow cytometry[28]. The data acquired by flow cytometry was analyzed using the FlowJo software v7.6 (FlowJo LLC, USA).

Determination of IFN-γ and IL-4 levels by ELISA

To quantitatively assess the precise impact of MCF-7 EVs on secretion of IFN-γ and IL-4 from PBMCs obtained from breast cancer patients, ELISA technique was recruited. In short, 0.7-1 × 10^6 patients' PBMCs were seeded into 48 well plates containing 80 mL of RPMI and 20 % exosome-free FBS. Upon 24 h of incubation at 37 °C, 5 µg/mL of phytohemagglutinin (PHA) (Invitrogen, USA) and 1, 2 or 5 µg of MCF-7 derived EVs were added into the conditioned media. After 48 h, the conditioned media were collected, and the supernatants were used for determination of IFN-γ and IL-4 levels. This assay was performed using the IFN-γ and IL-4 human ELISA kit (Invitrogen, Austria). The absorbance of the samples was read using a spectrophotometer (BioTek, USA) at a wavelength of 450 nm. A standard curve was plotted using the lyophilized IFN-γ and IL-4 proteins included in the ELISA kits.

Flow cytometry analysis to quantify Tregs population percentage

To explore the effect of breast cancer-derived EVs on the population of Treg cells, flow cytometry was also employed. For this purpose, patients' PBMC cells were treated with 1 µg of MCF-7 cells derived EVs for 48 h at 37 °C. Treated and untreated PBMCs were re-suspended in PBS and further incubated at 4 °C for 30 min with specific antibodies against Tregs, including CD4-FITC (357405, Bio legend, USA), CD25-APC (356109, Bio legend, USA) and FOXP3-PE (320207, Bio legend, USA) in 1:50 ratio of each. To determine the relative ratio of Tregs, the $CD4^+$ population was gated, followed by the $CD25^+$ $FOXP3^+$ population. Treg analysis was carried out with

a BD FACS Calibur (BD Biosciences, USA) and data were processed by the FlowJo software v7.6 (FlowJo LLC, USA).

PD-1 and PD-L1 expression levels assessed by flow cytometry

Examination of the expression levels of PD-1 and PD-L1 on PBMCs cell surface was conducted by incubation of the untreated and treated PBMCs with 1 µg of MCF-7 cells derived EVs using either of the monoclonal antibodies PD-1-FITC (621611, Biolegend, USA) and PD-L1- PerCP/Cyanine5.5 (329737, Biolegend, USA) each in 1:50 ratio. Flow cytometry was performed on a BD FACS Calibur (BD Biosciences, USA) and the data were analyzed with the FlowJo software v7.6 (FlowJo LLC, USA).

RNA extraction, cDNA synthesis and qRT-PCR analysis

To quantify the expression level of immune regulatory genes in patients' PBMCs, 1 µg of MCF-7 cells derived EVs were co-incubated with PBMCs for 48 h at 37 °C. Following incubation, total RNA was extracted from MCF-7 cells, untreated and treated PBMCs as well as EVs derived from MCF-7 cells using TrizolEX (DNAbiotech, Iran) according to the manufacturer construction, and finally stored at -80 °C. The quality and quantity of all the extracted RNAs were evaluated using nanodrop (BioTek, USA). Equal amounts of each RNA sample were used for cDNA synthesis (Sinaclon, Iran). Specific cDNA was prepared for miR-27a-3p and U6 snRNA using specific stem-loop primers, and random hexamer primers were used for cDNA synthesis of *Tbet*, *GATA3*, *FOXP3*, *PTEN*, *B2M* and *GAPDH* mRNAs. The cDNA samples were subjected to qRT-PCR using the SYBR Green 2X Real-time PCR Kit (Amplicon, Denmark) to evaluate the expression level of the above genes in samples. Furthermore, RealQ Plus 2x Master Mix for Probe (Amplicon, Denmark) was applied to assess the level of miR-27a-3p and U6 snRNA in MCF-7 cells, EVs and PBMCs as well. All PCR reactions were carried out in duplicates or triplicates using the Applied Biosystems StepOnePlus Real-Time PCR system (Thermo Fisher Scientific, Waltham, MA, USA). The data were collected and analyzed by StepOne Software v2.3 (Applied Biosciences, Thermo Fisher Scientific, Waltham, MA, USA). The relative levels of miRNA and mRNAs were standardized by comparing them to

the expression level of *GAPDH* or *B2M* for *Tbet*, *GATA3*, *FOXP3* and *PTEN* or U6 for miR-27a-3p through the $2^{-\Delta Ct}$ or $2^{-\Delta\Delta Ct}$ method to measure the fold change of the target genes expression in the samples. The sequences of probe, stemloop primers, forward and reverse primers are reported in Table 1.

Table 1. The primer sequences used in qRT-PCR of the target mRNAs and microRNAs

Name	*Sequence (5'-3')*
GATA3 F	TCATTAAGCCCAAGCGAAGG
GATA3 R	GTCCCCATTGGCATTCCTC
Tbet F	AAGTGGGTGCAGTGTGGAAA
Tbet R	TGGAGCACAATCATCTGGGT
FOXP3 F	CCTACGCCACGCTCATCC
FOXP3 R	CATTGAGTGTCCGCTGCTTC
GAPDH F	AGAAGGCTGGGGCTCATTTG
GAPDH R	TGGAGGAGGCATTGCTGATG
PTEN F	GAACAAGATGCTAAAAAAGGACAAAATG
PTEN R	CACGCTCTATACTACAAATGCTATCG
B2M F	AGATGAGTATGCCTGCCGTGT
B2M R	TGCGACATCTTCAAACCTCCAT
hsa-miR-27a-3p stem loop	GGTCGTATGCAAAGCAGGGTCCGAGGTATCCATCGCACGCATC GCACTGCATACGACCGCGGAA
U6 stem loop	GGTCGTATGCAAAGCAGGGTCCGAGGTATCCATCGCACGCATC GCACTGCATACGACCAAAATA
hsa-miR-27a-3p F	CATGCATTCACAGTGGCTAAGTTC
U6 F	CATCCAAAGGATGACACGCAAATTC
Universal Reverse primer	GCAAAGCAGGGTCCGAGG
Universal Probe	6FAM TCCATCGCACGCATCGCACT BHQ-1

Bioinformatics analysis

Data sources and processing

Gene expression profiles were retrieved from the gene expression omnibus (GEO) database (http://www.ncbi.nlm.nih.gov, accessed in September 2023). GSE27562 and GSE83669 datasets were selected to identify miRNA-mRNA regulatory modules in breast cancer. The GSE27562 was a microarray gene expression dataset in PBMCs of breast tumors (defined as cancer group) and healthy individuals (defined as control group). The GSE83669 dataset used next-generation small RNA sequencing to profile cellular and exosomal miRNA in human normal mammary gland epithelial cell line (MCF-10) and breast cancer cell line (MCF-7). The raw data was analyzed using GEO2R to discover the deferentially expressed genes (DEGs) and miRNAs (DEMs) between the two groups in each dataset. DEGs were defined by the adjusted *P*-value < 0.05. The mRNA targets of the DEMs were retrieved using the miRTarBase database[29]. The shared genes between DEMs targets and DEGs were found using Venn diagram (https://bioinfogp.cnb.csic.es/tools/venny, version 2.1) and subjected for further analyses.

Constructing the protein–protein interaction PPI network, screening the modules and identifying the miRNA-mRNA regulatory network

To establish PPI network, STRING db (https://string-db.org) was applied and a confidence score was set to medium = 0.7. PPI network visualization and analysis were performed using Cytoscape 3.7.1 software. To gain insight into significant biological clusters, the Molecular Complex Detection (MCODE) Cytoscape plugin was employed according to the following criteria: “Degree cutoff = 2”, “node score cutoff = 0.2”, “k-core = 2” and “max. Depth = 100”. Moreover, the interaction between selected miRNA and mRNA was identified using miRTarBase, the largest database containing experimentally validated miRNA-target interaction[29], to investigate the probable mechanisms involved in immune system regulation in breast cancer.

Functional enrichment analysis and hub gene screening

Each cluster was further analyzed using g:profiler website (https://biit.cs.ut.ee/gprofiler) to elucidate the biological function of the shared genes. Gene ontology (GO) analysis including molecular function (MF), biological process (BP), and cellular component (CC) as well as Reactome pathway were utilized. Statistical significance was defined as a *P*-value < 0.05. Genes with high closeness, betweenness centrality and neighborhood connectivity (degree) were considered as hub genes.

Statistical analysis

The statistical analysis was carried out utilizing a proprietary software (Prism 8.4.3; GraphPad Software, USA). Data analysis involved the application of *t*-test for comparing the difference between two groups and one-way analysis of variance for more than two groups. Results were expressed as mean ± standard error of the mean (SEM). Statistical significance was determined (*) for *p* values less than 0.05.

Graphical contents

All graphical contents showed in this study were original and prepared by Bio render and Abode illustrator (Adobe Illustrator 2020, USA).

RESULTS

Isolation and characterization of MCF-7 derived EVs

MCF-7 derived EVs were well isolated from the cell culture media according to the previously described protocol in methods. Then, EVs features such as the morphology and size distribution were evaluated by DLS and TEM techniques. As shown in Figure 2A, the isolated particles from the cell culture media demonstrated 2 peaks at 225.9 and 62.50 nm in terms of intensity; however, based on the particle number, most of the isolated particles were in size of 43.33 nm. In addition, the results from TEM imaging revealed the cup-shaped nanostructure of the isolated vesicles with an integrated bilayer membrane [Figure 2B]. Both TEM imaging and DLS analysis verified that the size distribution and morphology of the isolated particles fall within the typical range designated for EVs. Moreover, flow cytometry and western blot analysis corroborated the presence of EV markers in the isolated vesicles. Figure 2C

showed that TSG 101 as a positive EV marker was found in MCF-7 derived EVs, whereas Calnexin as a non-small EV marker was not detected[30]. As illustrated in Figure 2D, surface markers including CD9, CD63 and CD81 were detected in 52.15, 55.95 and 54.95% of the EVs, respectively. Overall, flow cytometry and western blot analysis confirmed the identity of the isolated vesicles through the presence of EV markers (CD9, CD63, CD81 and TSG101) and absence of negative EV marker (Calnexin).

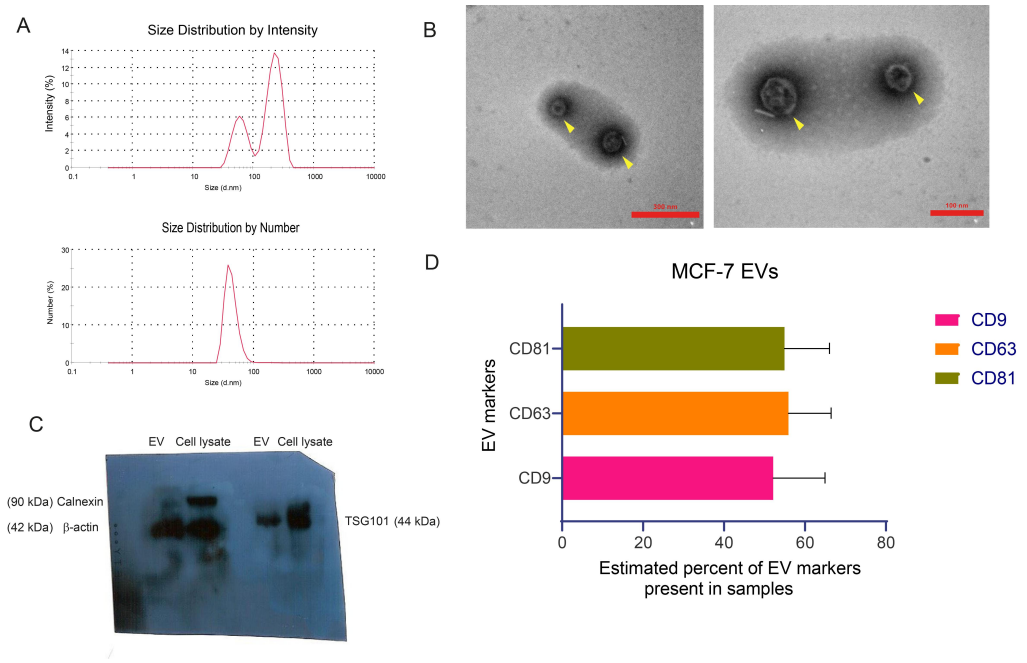

Figure 2. Characterization of the isolated EV-enriched fractions. A) Dynamic light scattering of the EVs indicating 2 peaks at 225.9 and 62.50 nm in terms of intensity and number; B) Transmission electron microscopy of MCF-7-derived EVs. Arrows indicate EVs with a cup-shape morphology (scale bar = 100 nm and 300 nm); C) Western blot analysis of the specific luminal protein markerTSG101, and Calnexin as a negative EV marker as well as β-actin as internal control. D) Flow cytometry analysis of EVs surface markers (CD9, CD63, CD81) calculated from the difference between EV counts.

Breast cancer-derived EVs were uptaken by PBMCs, predominantly monocytes

To explore whether EVs could be uptake by PBMCs, confocal microscopy was employed to visualize the PKH26 labelled-EVs internalization. Our results unveiled that the labeled MCF-7 EVs were efficiently taken up by PBMCs [Figure 3A]. To understand whether PKH-EVs were internalized into lymphocytes or monocytes, flow cytometry was applied. As the representative flow cytometry data shows in Figure 3B, 24 h after addition of the labelled MCF-7 EVs, a large proportion of monocytes were positive for PKH EVs, while lymphocytes were unable to uptake EVs (5.88 ± 0.3% *vs.* 0.11 ± 0.05 %, $p < 0.01$). Both confocal images and flow cytometry results demonstrated that EVs bind to the monocytes and are predominantly phagocytized by them.

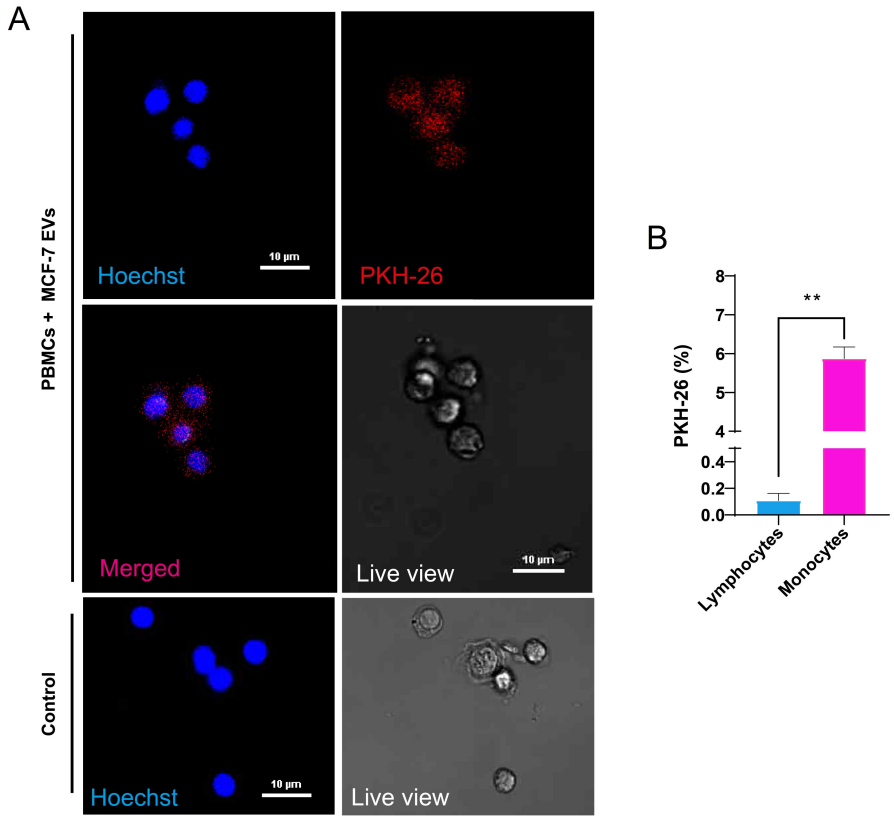

Figure 3. Internalization of MCF-7-derived EVs into PBMCs. A) Confocal fluorescence microscopy was used to observe the uptake of PKH-26 labeled EVs by PBMCs (scale bar = 10 µm); B) Quantifying the percentage of the PKH-26 labeled EVs internalized into the lymphocytes or monocytes subpopulations of PBMCs. $**p < 0.01$ compared between lymphocytes and monocytes.

Breast cancer cells EVs affected the immune response in ER+/PR+ patients' PBMCs

To evaluate the effect of EVs on patients' PBMCs immune function, and to observe the immunophenotypic alterations of PBMCs, they were pre-stimulated with PHA and then treated with 1, 2, and 5 µg of EVs obtained from MCF-7 cells, for 48 h. Our ELISA results revealed a significant decrease in the level of IFN-γ as an indicative of Th1 cells, upon treatment with all the EVs quantities used in this study when compared with PBMCs alone [Supplementary Figure 1]. A remarkable change in the amount of the secreted IFN-γ was observed after treatment with 1 µg of EVs, thus, 1 µg of MCF-7-derived EVs was selected for further experiments. Besides, as only a low alteration in the IL-4 level was detected by ELISA in the supernatant of PBMCs [Supplementary Figure 2], we performed q-RT PCR to investigate the GATA3, Th2 gene hallmark, to improve the sensitivity in detecting the Th2 cell marker. To do this, we co-incubated 1 µg of EVs with 1×10^6 of PBMCs, pre-stimulated with PHA, and then divided them into the treated and untreated groups. Cell culture media were collected for ELISA assay and the remaining PBMCs underwent flow cytometry and qRT-PCR analysis. The data from the ELISA assay displayed a significantly diminished level of IFN-γ in the treated PBMCs [Figure 4A]. To further track the immunophenotypic change in PBMCs, we decided to measure the Treg cell population following exposure to 1 µg of EVs. Representative flow cytometry data illustrates no statistically significant difference in $CD4^+CD25^+FOXP3^+$ Tregs frequency between the untreated and treated groups [Figure 4B].

Additionally, to evaluate the immunological impact of EVs on patients' PBMCs at the RNA level, qRT-PCR was employed to investigate the expression levels of T lymphocyte-specific gene markers, including T-bet, GATA3, and FOXP3. Our findings indicated that co-incubation of 1 µg of breast cancer-derived EVs with PBMCs obtained from ER+/PR+ breast cancer patients, resulted in a significant decrease in the level of T-bet, a hallmark of Th1 cells. On the contrary, a significant elevation in the levels of GATA3 and FOXP3, serving as individual markers for Th2

and Treg cells, was found reflecting an imbalance between Th1, Th2 and Treg cells, thereby affecting the composition of the immune cells in response to tumor-derived EVs [Figure 4C].

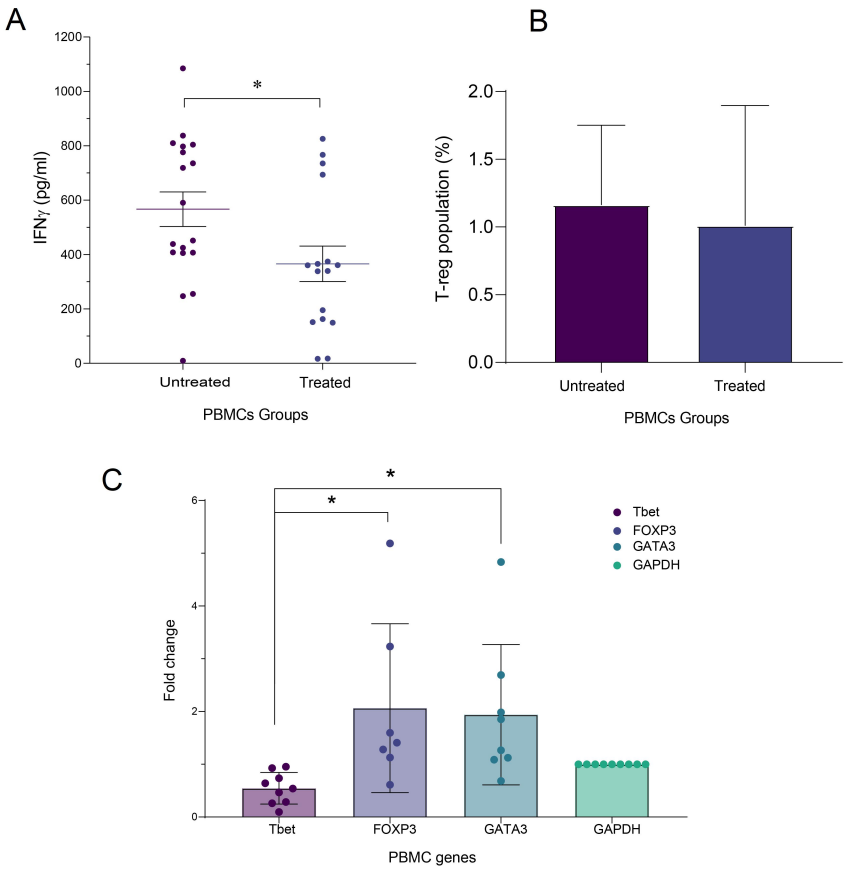

Figure 4. Immunomodulatory effects of MCF-7 derived EVs (1µg) on ER+/PR+ breast cancer patients' PBMCS. A) ELISA assay was applied to measure the level of the secreted IFN-γ into cell culture media; B) Assessment of alteration in T reg subpopulation using the flow cytometry technique; C) qRT-PCR results show the effect of EVs on the fold change of Tbet, GATA3 and FOXP3 expression in PBMCs. GAPDH was measured as an internal control. One way ANOVA analysis and *t*-test were used to show the significant difference between multiple and two groups, respectively. $^{*}p < 0.05$ compared to untreated PBMCs.

To study whether PD-1/PD-L1 axis is responsible for disturbing the lymphocyte subpopulation balance, the biological implication of MCF-7-derived EVs on PBMCs

was analyzed using flow cytometry. Based on these findings, the expression of surface PD-1 on the PBMCs was augmented following treatment with EVs relative to the untreated ones [Figure 5A]. Interestingly, we found an overexpression in the level of PD-L1 on the surface of the monocyte subpopulation of PBMCs [Figure 5B].

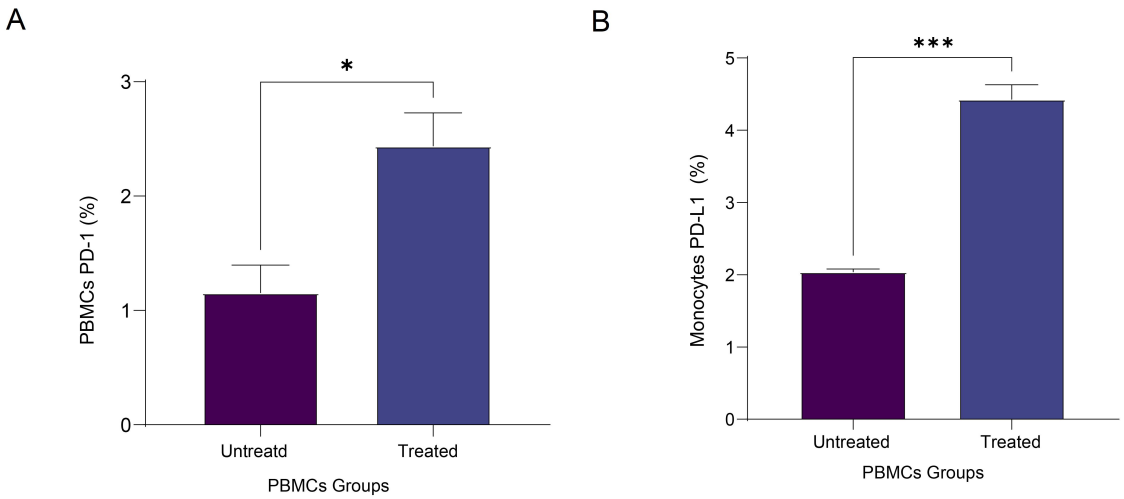

Figure 5. Evaluating the percentage of A) PD-1 and B) PD-L1 present in PBMCs and monocyte subpopulation after 48 h of incubation with 1µg of EVs using flow cytometry. $^{*}p < 0.05$ and $^{***}p < 0.001$ compared with the untreated PBMCs. Each data represent mean±SEM of at least three replicates.

Bioinformatics analysis showed that EVs miR-27a-3p targets PTEN gene in PBMCs of ER+/PR+ breast cancer patients

According to the gene expression analysis, 8595 DEGs and 128 DEMs were identified in PBMCs and EVs, respectively. The targets of DEMs in MCF-7-derived EVs, identified by miRTarBase, were then compared with robust DEGs in breast cancer patients' PBMCs via Venn diagram. Among them, 1,452 genes were found to be overlapped [Figure 6A]. These shared genes were selected to construct the PPI network and identify the clusters of biological pathways. MCODE analysis dissected the PPI network into 4 significant biological clusters with scores > 6 and node numbers > 20. Thereafter, GO term annotation and pathway analysis were performed. Top 10 GO terms and pathways, selected based on the -$\log_{10}P$-value, were illustrated in Figure 6B. The clustered 1,452 genes were analyzed to

discover the genes that were potentially contributed to cancer or immunological pathways. Enrichment pathway analysis explored several pathways related to interleukin and cytokine signaling in cluster A. Of note, in cluster A, PI3K/AKT is the most significant pathway which has a critical role in cell proliferation, angiogenesis, apoptosis, and EMT[31]. Furthermore, clusters B, C and D included the genes that were significantly associated with cell cycle, mitochondria and metabolisms along with innate immune system pathways, respectively [Figure 6B , Supplementary Figure 3].

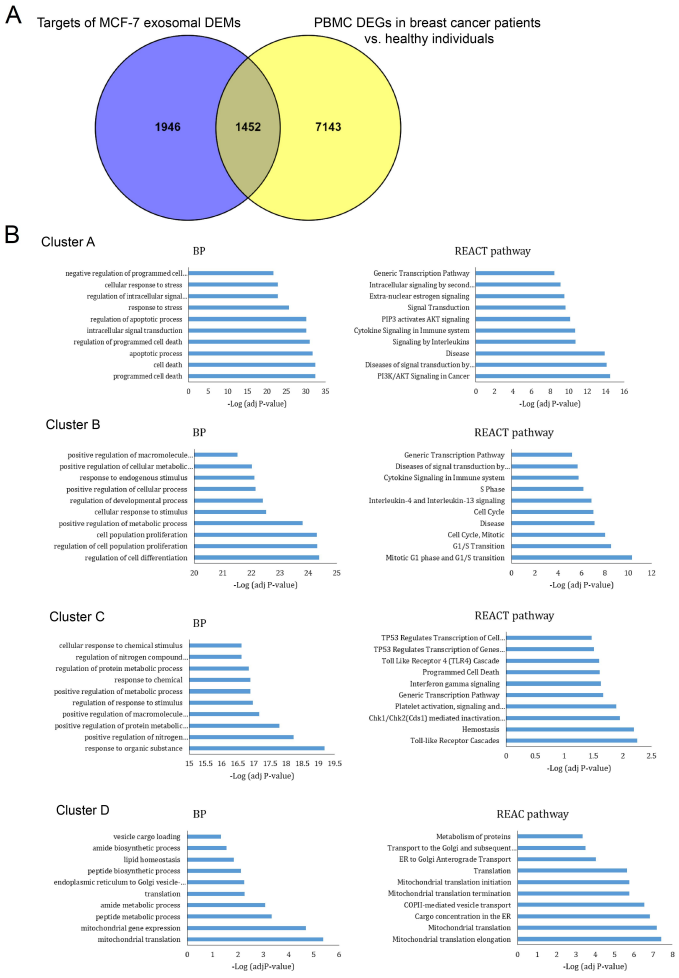

Figure 6. Representative data from bioinformatics. A) Overlapped common genes. Venn diagram compared targets of DEMs in MCF-7 EVs and DEGs in PBMCs. DEM differentially expressed miRNAs; DEGs, differentially expressed genes; B) biological process (BP) ontology and signaling pathways (REAC). Four significant biological

clusters were identified by g:profiler and then analyzed for GO enrichment. Top 10 GO terms were represented in clusters A to D respectively.

We then developed a miRNA-gene regulatory interaction network because of the important role of miRNA-gene interaction in different cellular functions. As shown in Table 2, the 14 hub genes, chosen based on the centrality parameter, were primarily involved in cell cycle progression and immune system. Among them, PTEN has been well established as a tumor suppressor gene that inhibits PI3K/AKT signaling pathway and negatively regulates the programmed cell death ligand 1 (PD-L1) gene expression in macrophages[25]. Keeping in mind that PD-L1 is an immune checkpoint with a critical role in immune evasion[32], our in-silico analysis of GSE27562 dataset revealed that PTEN expression is down-regulated in PBMCs of the patients suffering from breast cancer compared to healthy individuals. Interestingly, various DEMs in MCF-7-derived EVs such as miR-27a/23a could target PTEN [Figure 7A] along with GATA3 and FOXP3 [Figure 7B] in our analysis. In this context, evidence unraveled the role of miR-27a/23a in tumor progression and metastasis in different types of cancers including hepatocellular carcinoma, breast cancer, and colorectal cancer[25,33-35]. Given these data and considering a previous study demonstrating that miR-27a-3p could positively regulate PD-L1 through PTEN, we decided to experimentally verify the expression level of miR-27a and its target PTEN in MCF-7-derived EVs and EVs-treated PBMCs.

Table 2. Hub genes in cluster 1 involved in the regulation of breast cancer immune system.

Gene name	Uniprot ID	Function	Degree
CCND1	P24385	Regulatory component of the cyclin D1-CDK4 (11) complex	60
GAPDH	P04406	A key enzyme in glycolysis	59
PARP1	P09874	Poly-ADP-ribosyltransferase mediating poly-ADP-ribosylation of proteins	58
PTEN	P60484	Inhibits the PI3K-AKT/PKB signaling pathway through	56

		dephosphorylation of the phosphoinositides and thereby influencing cell cycle progression and cell survival	
ATM	Q13315	Plays a role in pre-B cell allelic exclusion and in T-cell development	55
SRC	P12931	Contributes in signaling pathways that control a variety of biological functions including gene transcription, immune response, cell adhesion, cell cycle progression, apoptosis, migration, and transformation	54
CDH1	P12830	Regulating cell-cell adhesions, mobility and proliferation of epithelial cells	54
CTNNB1	P35222	Key downstream component of the canonical Wnt signaling pathway, regulation of T cell proliferation	54
ERBB2	P04626	Regulation of T cell proliferation and differentiation	53
HIF1A	Q16665	Acts as a master transcriptional regulator of the adaptive response to hypoxia, induces expression of ACE2 and cytokines such as IL1B, TNF, IL6, and IFNs in monocytes,	53
E2F1	Q01094	Transcription activator that binds to DNA	52
GSK3B	P49841	Activation of the protein kinase, as a negative regulator in the hormonal control of glucose homeostasis, Wnt signaling, Phosphorylates SFPQ at ‘Thr-687’ upon T-cell activation	52
MDM2	Q00987	Ubiquitinates p53/TP53 which results in its degradation by the proteasome	51
CDKN1B	P46527	Important regulator of cell cycle progression	46

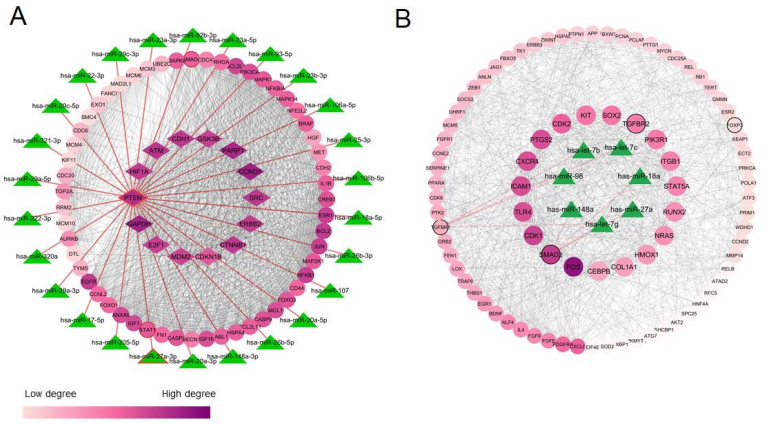

Figure 7. The mRNA-miRNA regulated network. A) The putative mechanism for PD-L1 expression regulation in cluster 1; B) The suggested mechanism for regulation of FOXP3 expression in cluster2. DEMs in MCF-7-derived EVs (green triangle) could potentially target DEGs in breast cancer PBMCs. The hub genes are shown in diamond and other DEGs in circle.

EVs miR-27a-3p diminished PTEN gene expression in PBMCs in upstream of PD-L1 pathway

Building on our bioinformatics data, we further assessed the relative expression of *PTEN* gene in patients' PBMCs prior to and post EVs incubation and also miR-27a-3p expression in the breast cancer derived EVs compared to their parent cells, MCF-7. Our observations demonstrated that the level of hsa-miR-27a-3p in the MCF-7-derived EVs was significantly over-expressed in comparison to MCF-7 cells which agrees with our bioinformatics findings [Figure 8A]. Furthermore, we detected an elevated expression level of hsa-miR-27a-3p in ER+/PR+ breast cancer patients' PBMCs upon 48 h of co-incubation with MCF-7-derived EVs, highlighting our recent findings, where EVs were uptake by PBMCs [Figure 8B]. Moreover, the expression level of *PTEN* as a target gene for miR-27a-3p, was measured by qRT-PCR. We found a reduction in the expression level of *PTEN* in patients' PBMCs following incubation with EVs [Figure 8C].

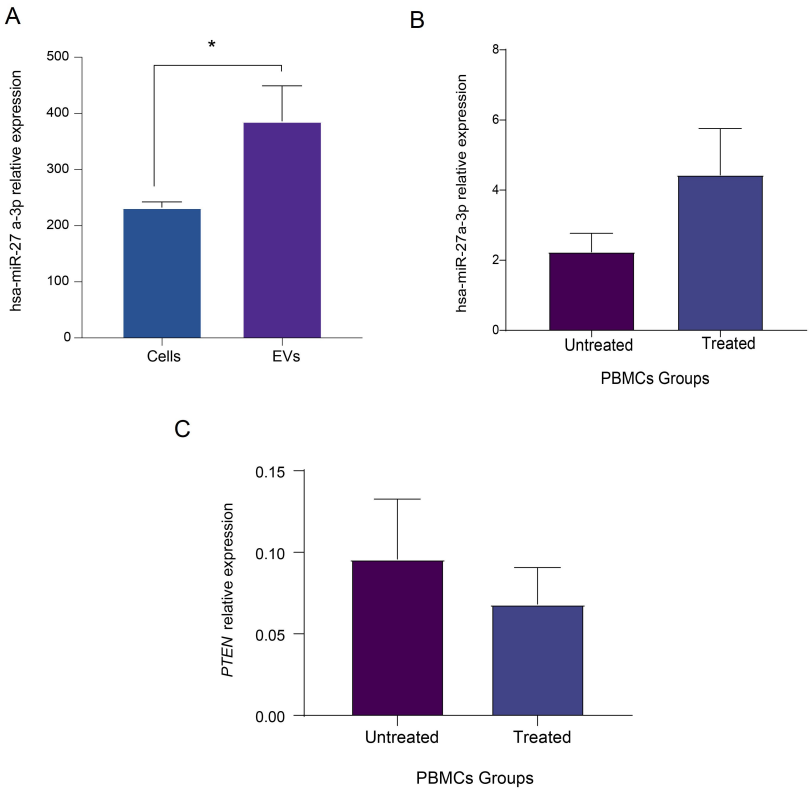

Figure 8. Validation of bioinformatics outcomes. A) The relative expression of miR-27a-3p was assessed in MCF-7 cells and the secreted EVs using qRT-PCR. The Relative expression of B) miR-27a-3p and C) PTEN was assessed in the untreated and treated PBMCs with 1µg of EVs using qRT-PCR. t-test analysis showed a difference in the expression level of target genes between the two groups.

DISCUSSION

Understanding the role of EVs in modulating the cellular composition of TIME would help to close our current knowledge gaps in cancer biology[30]. EVs are able to traverse biological barriers and have dynamic regulation in response to alterations in immuno-pathological states of individuals[36,37]. These features along with their pervasive presence render them not only essential mediators of cancer progression but also outstanding biomarkers, which reshape our comprehension of intercellular communication in the context of cancer immunology[38,39]. Due to inconsistent findings of immunomodulatory function of EVs in breast cancer, studies on crosstalk

between breast cancer- derived EVs and immune cells present in TIME composition, have emerged.

Here in this work, we attempted to investigate the immunomodulatory impact of breast cancer derived-EVs on the PBMCs collected from women who were diagnosed with non-metastatic ER+/PR+ breast cancer. Characteristically, DLS and TEM results approved the shape and size of the isolated EVs. Meanwhile, specific markers of EVs recommended by ISEV such as CD9, CD63, CD81 and TSG101 were well detected in the EVs derived from MCF-7 cells using Western blot analysis and flow cytometry[30]. We also witnessed that PKH-26-labeled EVs were well up-taken by PBMCs using confocal microscopy. Furthermore, most of these EVs were found to be phagocytized by monocytes as revealed by flow cytometry data.

Previous studies have reported that EVs secreted by breast cancer cells into the circulatory system, stimulate macrophages via the NF-κB signaling pathway leading to a pro-inflammatory activity[40]. In addition to their role in macrophage polarization, cancer derived EVs contribute to all types of immunological pathways[41-43]. Hellwinkel *et al.* discovered that glioma-derived EVs suppress IFN-γ secretion from PBMCs, nonetheless this output was dependent on the concentration of EVs[44]. In addition, breast cancer derived EVs were reported to induce T regulatory cells and promote their differentiation through TGF-β1/SMAD5 signaling pathway activation[45]. Furthermore, Huang and his colleagues demonstrated that the EVs isolated from dendritic cells caused an elevation in the level of IL-4 and a reduction in those of IFN-γ, leading to the promotion of Th2 cells[46]. Based on these enthusiastic findings, we decided to unravel the potential of breast cancer-EVs to modulate the immune responses in the PBMCs of ER+/PR+ breast cancer patients. To validate this hypothesis, here in this study, we first noticed that 1μg of cancerous EVs efficiently reduced the level of IFN-γ, an indicator for Th1 cells activity, in the PBMCs pre-stimulated with PHA[47,48]. However, this quantity of EVs was insufficient to change the frequency of $CD25^{+}FOXP3^{+}$Tregs population within ER+/PR+ PBMCs. Of note, the level of IL-4 did not alter in both EVs-treated/untreated PBMCs. Owing to the

discrepancies observed between our data and those of others regarding the promotion of Tregs and Th2 cells in the presence of EVs, we set to monitor the expression levels of Th1, Th2 and Treg genes hallmarks. To our surprise, 1µg of cancerous EVs was capable of elevating the expression of *GATA3* and *FOXP3* as specific gene markers for Th2 and Treg, respectively, as well as lowering those of the Th1 specific gene marker, *Tbet*. These findings suggest that breast cancer-derived EVs might induce a skew in the balance among Th1, Th2 and Treg cell populations, eventually leading to an immune suppression that facilitates tumor growth[49-51].

Studies have shown a correlation between PD-1$^+$ T cell population and anti-tumor immunity[52-54]. It is worth mentioning that exosomal tumor cells evade immune surveillance by activating the PD-1 inhibitory pathway in T cells, thereby facilitating tumor growth[54,55]. On the other hand, a marked elevation of PD-L1 expression has been found to promote tumor growth through binding to PD-1 receptor on T cells, resulting in the inability of T cells[56,57]. In agreement with these data, we found that phagocytosis of breast cancer-derived EVs caused a significant rise in the levels of PD-L1 on the monocyte subpopulation of PBMCs and subsequently attached to the activated T cells expressing PD-1 on the surface, which is in favor of tumor progression.

Through further research on the role of EVs in tumor growth, it has been revealed that EVs are a package containing a wide range of components, which act in message transmission and intracellular communication[58]. Among them, microRNAs (miRNAs) are the most abundant cargos contributing to breast cancer development by modulating the function of immune cells[59]. It is well documented that target genes of miRNAs function through a network by interacting with other molecules[60]. In this context, systems biology is an approach by which the regulatory roles of miRNAs in a network could be elucidated[60]. Hence, we were encouraged to answer this key question whether EV miRNAs can modulate the immune response leading to breast cancer progression. Our results showed an elevated expression of miR-27a-3p in the EVs derived from MCF-7 cells relative to their parent cells, a finding consistent with

previous reports introducing miR-27a-3p as an indicator of breast cancer exosomal miRNA[61,62]. Interestingly, data from the systems biology revealed that miR-27a-3p modulates PD-L1, *FOXP3* and *GATA3* expression through PTEN. Furthermore, we detected an enhanced level of miR-27a-3p in the patients' PBMCs following incubation with EVs, implying the EVs uptake by PBMCs. Consistently, a study performed by Yao *et al.* detected an up-regulation of breast cancer cell exosomal miR-27a-3p, which caused PD-L1 overexpression in macrophages via *PTEN* gene, thereby promoting immune evasion of breast cancer cells[25]. Given these data and knowing that EVs were unable to enter T cells and were mainly phagocytized by the monocyte subpopulation, we suggest that breast cancer-derived EVs have likely participated in ER+/PR+ breast cancer development following immune escape via PD-L1/PD-1 pathway, which in turn influences Th2 and Tregs activity. In parallel, we found an elevated expression level of *PTEN* gene in patients' PBMCs following internalization of the breast cancer EVs expressing miR-27a-3p, which might be independent of the PDL1 axis.

CONCLUSION

In conclusion, the present study provides new insights into how EVs derived from MCF-7 cells and up-taken by the monocyte subpopulation of ER+/PR+ breast cancer patients' PBMCs, cause a skew in the balance of immune cells population including Th1, Th2 and Tregs by likely triggering the PDL-1/PD-1 signaling pathway. Our results also suggest that the exosomal miR-27a-3p might be responsible for this immunoregulation via *PTEN* gene; however, more clinical samples and further experimental studies are required to validate these findings. Finally, our results might help direct the future development of novel theranostic targets for breast cancer.

DECLARATIONS

Authors' contributions

Performed all experiments and prepared a draft of manuscript and Assisted in the biological experiments: A.T.G;

Performed and interpreted the bioinformatics data: R.D;

Assisted in molecular genetic analysis: A.R. and M.K;

Provided the patients' samples: A.M;

Analyzed the data, edited the manuscript and provided suggestions to improve the work: S.I. and A.N;

Assisted in study design and edited the manuscript: A.C.T;

Designed the study, provided the financial support and suggestions to improve the work, and edited the manuscript: M.S.

Availability of data and materials

All relevant data can be found in the manuscript and supplement. Data are also available from the corresponding author upon reasonable request.

AI and AI-assisted tools Statement

The authors declared that generative AI was not used in the creation of this manuscript.

Financial support and sponsorship

This work was financially supported by grants from Pasteur Institute of Iran (#1145), and the Iran National Science Foundation (# 99008672).

Conflict of interest

The authors declare that they have no competing interests.

Ethical approval and consent to participate

Study was acknowledged by the Ethics Committee of Pasteur Institute of Iran (ethical code: IR.TUMS.HORCSCT.REC.1400.029).

Consent for publication

Not applicable.

Copyright

REFERENCES

1. Demuytere J, Ernst S, van Ovost J, Cosyns S, Ceelen W. Chapter Four - The tumor immune microenvironment in peritoneal carcinomatosis. In: Aranda F, Berraondo P, Galluzzi L, editors. International Review of Cell and Molecular Biology. 371: *Academic Press;* 2022. p. 63-95.[DOI: 10.3390/cancers17193217]

2. Binnewies M, Roberts EW, Kersten K, et al. Understanding the tumor immune microenvironment (TIME) for effective therapy. *Nat Med.* 2018;24(5):541-50.[PMID: 29686425 PMCID: PMC5998822 DOI: 10.1038/s41591-018-0014-x]

3. Amens JN, Bahçecioglu G, Zorlutuna P. Immune System Effects on Breast Cancer. *Cell Mol Bioeng.* 2021;14(4):279-92.[PMID: 34295441 PMCID: PMC8280260 DOI: 10.1007/s12195-021-00679-8]

4. Rajbhandary S, Dhakal H, Shrestha S. Tumor immune microenvironment (TIME) to enhance antitumor immunity. *Eur J Med Res.* 2023;28(1):169.[PMID: 37179365 PMCID: PMC10182604 DOI: 10.1186/s40001-023-01125-3]

5. Zhou C, Liu Q, Xiang Y, Gou X, Li W. Role of the tumor immune microenvironment in tumor immunotherapy. *Oncol Lett.* 2022;23(2):53.[PMID: 34992685 PMCID: PMC8721848 DOI: 10.3892/ol.2021.13171]

6. Lee H, Na KJ, Choi H. Differences in Tumor Immune Microenvironment in Metastatic Sites of Breast Cancer. *Front Oncol.* 2021;11:649004.[PMID: 33816302 PMCID: PMC8013993 DOI: 10.3389/fonc.2021.649004]

7. Pérez-Romero K, Rodríguez RM, Amedei A, Barceló-Coblijn G, Lopez DH. Immune Landscape in Tumor Microenvironment: Implications for Biomarker Development and Immunotherapy. *Int J Mol Sci.* 2020;21(15).[PMID: 32752264 PMCID: PMC7432816 DOI: 10.3390/ijms21155521]

8. Baxevanis CN, Fortis SP, Perez SA. The balance between breast cancer and the immune system: Challenges for prognosis and clinical benefit from immunotherapies. *Semin Cancer Biol.* 2021;72:76-89.[PMID: 31881337 DOI: 10.1016/j.semcancer.2019.12.018]

9. Li L, Yang C, Zhao Z, Xu B, Zheng M, Zhang C, et al. Skewed T-helper (Th)1/2- and Th17/T regulatory-cell balances in patients with renal cell carcinoma. *Molecular medicine reports.* 2014;11.[PMID: 25352158 PMCID: PMC4262517 DOI: 10.3892/mmr.2014.2778]

10. Ciarka A, Piątek M, Pęksa R, Kunc M, Senkus E. Tumor-Infiltrating Lymphocytes (TILs) in Breast Cancer: Prognostic and Predictive Significance across Molecular Subtypes. *Biomedicines [Internet].* 2024; 12(4).[PMID: 38672117 PMCID: PMC11048219 DOI: 10.3390/biomedicines12040763]

11. Denkert C, von Minckwitz G, Darb-Esfahani S, et al. Tumour-infiltrating lymphocytes and prognosis in different subtypes of breast cancer: a pooled analysis of 3771 patients treated with neoadjuvant therapy. *Lancet Oncol.* 2018;19(1):40-50.[PMID: 29233559 DOI: 10.1016/S1470-2045(17)30904-X]

12. Tower H, Ruppert M, Britt K. The Immune Microenvironment of Breast Cancer Progression. *Cancers (Basel).* 2019;11(9).[PMID: 31527531 PMCID: PMC6769749 DOI: 10.3390/cancers11091375]

13. Xu J, Gao F, Liu W, Guan X. Cell-cell communication characteristics in breast cancer metastasis. *Cell Communication and Signaling.* 2024;22(1):55.[PMID: 38243240 PMCID: PMC10799417 DOI: 10.1186/s12964-023-01418-4]

14. Salemme V, Centonze G, Cavallo F, Defilippi P, Conti L. The Crosstalk Between Tumor Cells and the Immune Microenvironment in Breast Cancer: Implications for Immunotherapy. *Frontiers in Oncology.* 2021;11.[PMID: 33777750 PMCID: PMC7991834 DOI: 10.3389/fonc.2021.610303]

15. Nicolini A, Ferrari P, Biava PM. Exosomes and Cell Communication: From Tumour-Derived Exosomes and Their Role in Tumour Progression to the Use of Exosomal Cargo for Cancer Treatment. *Cancers (Basel).* 2021;13(4).[PMID: 33669294 PMCID: PMC7920050 DOI: 10.3390/cancers13040822]

16. Krylova SV, Feng D. The Machinery of Exosomes: Biogenesis, Release, and Uptake. *Int J Mol Sci.* 2023;24(2).[PMID: 36674857 PMCID: PMC9865891 DOI: 10.3390/ijms24021337]

17. Hisey CL, Artuyants A, Guo G, et al. Investigating the consistency of extracellular vesicle production from breast cancer subtypes using CELLine adherent bioreactors.

Journal of Extracellular Biology. 2022;1(9):e60.[PMID: 38938775 PMCID: PMC11080891 DOI: 10.1002/jex2.60]

18. Tamrin SH, Phelps J, Nezhad AS, Sen A. Critical considerations in determining the surface charge of small extracellular vesicles. *J Extracell Vesicles.* 2023;12(9):e12353.[PMID: 37632212 PMCID: PMC10457570 DOI: 10.1002/jev2.12353]

19. Welsh JA, Goberdhan DCI, O'Driscoll L, et al. Minimal information for studies of extracellular vesicles (MISEV2023): From basic to advanced approaches. *J Extracell Vesicles.* 2024;13(2):e12404.[PMID: 38326288 PMCID: PMC10850029 DOI: 10.1002/jev2.12404]

20. Gharavi AT, Irian S, Niknejad A, Parang K, Salimi M. Harnessing exosomes as a platform for drug delivery in breast cancer: A systematic review for *in vivo* and *in vitro* studies. *Mol Ther Oncol.* 2024;32(2):200800.[PMID: 38706989 PMCID: PMC11067457 DOI: 10.1016/j.omton.2024.200800]

21. Knox MC, Ni J, Bece A, et al. A Clinician's Guide to Cancer-Derived Exosomes: Immune Interactions and Therapeutic Implications. *Front Immunol.* 2020;11:1612.[PMID: 32793238 PMCID: PMC7387430 DOI: 10.3389/fimmu.2020.01612]

22. Loconte L, Arguedas D, El R, et al. Detection of the interactions of tumour derived extracellular vesicles with immune cells is dependent on EV-labelling methods. *J Extracell Vesicles.* 2023;12(12):e12384.[PMID: 38031976 PMCID: PMC10687762 DOI: 10.1002/jev2.12384]

23. Jiang M, Zhang W, Zhang R, et al. Cancer exosome-derived miR-9 and miR-181a promote the development of early-stage MDSCs via interfering with $SOCS_3$ and $PIAS_3$ respectively in breast cancer. *Oncogene.* 2020;39(24):4681-94.[PMID: 32398867 DOI: 10.1038/s41388-020-1322-4]

24. Chen WX, Wang DD, Zhu B, et al. Exosomal miR-222 from adriamycin-resistant MCF-7 breast cancer cells promote macrophages M2 polarization via PTEN/Akt to induce tumor progression. *Aging (Albany NY).* 2021;13(7):10415-30.[PMID: 33752173 PMCID: PMC8064228 DOI: 10.18632/aging.202802]

25. Yao X, Tu Y, Xu Y, Guo Y, Yao F, Zhang X. Endoplasmic reticulum stress-induced exosomal miR-27a-3p promotes immune escape in breast cancer via regulating PD-L1 expression in macrophages. *Journal of Cellular and Molecular Medicine.* 2020;24.[PMID: 32672418 PMCID: PMC7520328 DOI: 10.1111/jcmm.15367]

26. Pospichalova V, Svoboda J, Dave Z, et al. Simplified protocol for flow cytometry analysis of fluorescently labeled exosomes and microvesicles using dedicated flow cytometer. *J Extracell Vesicles.* 2015;4:25530.[PMID: 25833224 PMCID: PMC4382613 DOI: 10.3402/jev.v4.25530]

27. Pužar Dominkuš P, Stenovec M, Sitar S, et al. PKH26 labeling of extracellular vesicles: Characterization and cellular internalization of contaminating PKH26 nanoparticles. *Biochimica et Biophysica Acta (BBA) - Biomembranes.* 2018;1860(6):1350-61.[PMID: 29551275 DOI: 10.1016/j.bbamem.2018.03.013]

28. Gonçalves FDC, Luk F, Korevaar SS, et al. Membrane particles generated from mesenchymal stromal cells modulate immune responses by selective targeting of pro-inflammatory monocytes. *Sci Rep.* 2017;7(1):12100.[PMID: 28935974 PMCID: PMC5608915 DOI: 10.1038/s41598-017-12121-z]

29. Huang HY, Lin YC, Li J, et al. miRTarBase 2020: updates to the experimentally validated microRNA-target interaction database. *Nucleic Acids Res.* 2020;48(D1):D148-54.[PMID: 31647101 PMCID: PMC7145596 DOI: 10.1093/nar/gkz896]

30. Théry C, Witwer KW, Aikawa E, et al. Minimal information for studies of extracellular vesicles 2018 (MISEV2018): a position statement of the International Society for Extracellular Vesicles and update of the MISEV2014 guidelines. *J Extracell Vesicles.* 2018;7(1):1535750.[PMID: 30637094 PMCID: PMC6322352 DOI: 10.1080/20013078.2018.1535750]

31. He Y, Sun MM, Zhang GG, et al. Targeting PI3K/Akt signal transduction for cancer therapy. *Signal Transduction and Targeted Therapy.* 2021;6(1):425.[PMID: 34916492 PMCID: PMC8677728 DOI: 10.1038/s41392-021-00828-5]

32. Lin X, Kang K, Chen P, et al. Regulatory mechanisms of PD-1/PD-L1 in cancers. *Molecular Cancer.* 2024;23(1):108.[PMID: 38762484 PMCID: PMC11102195 DOI: 10.1186/s12943-024-02023-w]

33. Quan J, Liu S, Dai K, et al. MicroRNA-23a/24-2/27a as a potential diagnostic biomarker for cancer: A systematic review and meta-analysis. *Mol Clin Oncol.* 2018;8(1):159-69.[PMID: 29387410 PMCID: PMC5769231 DOI: 10.3892/mco.2017.1492]

34. Cui M, Liu Z, Wang S, et al. CRISPR-based dissection of microRNA-23a ~ 27a ~ 24-2 cluster functionality in hepatocellular carcinoma. *Oncogene.* 2024;43(36):2708-21.[PMID: 39112518 PMCID: PMC11364504 DOI: 10.1038/s41388-024-03115-z]

35. Wang N, Tan H-Y, Feng Y-G, Zhang C, Chen F, Feng Y. microRNA-23a in Human Cancer: Its Roles, Mechanisms and Therapeutic Relevance. *Cancers [Internet].* 2019; 11(1).[PMID: 30577536 PMCID: PMC6356664 DOI: 10.3390/cancers11010007]

36. Xie F, Zhou X, Fang M, et al. Extracellular Vesicles in Cancer Immune Microenvironment and Cancer Immunotherapy. *Adv Sci (Weinh).* 2019;6(24):1901779.[PMID: 31871860 PMCID: PMC6918121 DOI: 10.1002/advs.201901779]

37. Buzas EI. The roles of extracellular vesicles in the immune system. *Nature Reviews Immunology.* 2023;23(4):236-50.PMID: 35927511 PMCID: PMC9361922 DOI: 10.1038/s41577-022-00763-8]

38. Li X, Liu Y, Zheng S, et al. Role of exosomes in the immune microenvironment of ovarian cancer (Review). *Oncol Lett.* 2021;21(5):377.[PMID: 33777201 PMCID: PMC7988709 DOI: 10.3892/ol.2021.12638]

39. Sohal IS, Kasinski AL. Emerging diversity in extracellular vesicles and their roles in cancer. *Front Oncol.* 2023;13:1167717.[PMID: 37397375 PMCID: PMC10312242 DOI: 10.3389/fonc.2023.1167717]

40. Zhou Q, Wang J, Zhang H, et al. Tumor-derived exosomes RNA expression profiling identifies the prognosis, immune characteristics, and treatment in HR+/HER2-breast cancer. *Aging (Albany NY).* 2023;15(16):8471-86.[PMID: 37647033 PMCID: PMC10497011 DOI: 10.18632/aging.204986]

41. Gharavi AT, Hanjani NA, Movahed E, Doroudian M. The role of macrophage subtypes and exosomes in immunomodulation. *Cellular & Molecular Biology Letters.* 2022;27(1):83.[PMID: 36192691 PMCID: PMC9528143 DOI: 10.1186/s11658-022-00384-y]

42. Ahmadi M, Abbasi R, Rezaie J. Tumor immune escape: extracellular vesicles roles and therapeutics application. *Cell Commun Signal.* 2024;22(1):9.[PMID: 38167133 PMCID: PMC10763406 DOI: 10.1186/s12964-023-01370-3]

43. Qiu H, Liang J, Yang G, et al. Application of exosomes in tumor immunity: recent progresses. *Frontiers in Cell and Developmental Biology.* 2024;12.[PMID: 38633106 PMCID: PMC11021734 DOI: 10.3389/fcell.2024.1372847]

44. Hellwinkel JE, Redzic JS, Harland TA, Gunaydin D, Anchordoquy TJ, Graner MW. Glioma-derived extracellular vesicles selectively suppress immune responses. *Neuro Oncol.* 2016;18(4):497-506.[PMID: 26385614 PMCID: PMC4799676 DOI: 10.1093/neuonc/nov170]

45. Ni C, Fang QQ, Chen WZ, et al. Breast cancer-derived exosomes transmit lncRNA SNHG16 to induce CD73+γδ1 Treg cells. *Signal Transduct Target Ther.* 2020;5(1):41.[PMID: 32345959 PMCID: PMC7188864 DOI: 10.1038/s41392-020-0129-7]

46. Huang L, Zhang X, Wang M, et al. Exosomes from Thymic Stromal Lymphopoietin-Activated Dendritic Cells Promote Th2 Differentiation through the OX40 Ligand. *Pathobiology.* 2019;86(2-3):111-7.[PMID: 30408778 DOI: 10.1159/000493013]

47. Lee JS, Song CH, Kim CH, et al. Profiles of IFN-gamma and its regulatory cytokines (IL-12, IL-18 and IL-10) in peripheral blood mononuclear cells from patients with multidrug-resistant tuberculosis. *Clin Exp Immunol.* 2002;128(3):516-24.[PMID: 12067307 PMCID: PMC1906259 DOI: 10.1046/j.1365-2249.2002.01858.x]

48. Kamimaki C, Kobayashi N, Hirata M, et al. T-cell response to phytohemagglutinin in the interferon-γ release assay as a potential biomarker for the response to immune checkpoint inhibitors in patients with non-small cell lung cancer. *Thoracic Cancer.* 2021;12(11):1726-34.[PMID: 33943031 PMCID: PMC8169292 DOI: 10.1111/1759-7714.13978]

49. Zhou J, Li X, Wu X, et al. Exosomes Released from Tumor-Associated Macrophages Transfer miRNAs That Induce a Treg/Th17 Cell Imbalance in Epithelial Ovarian Cancer. *Cancer Immunology Research.* 2018;6(12):1578-92.[PMID: 30396909 DOI: 10.1158/2326-6066.CIR-17-0479]

50. Lin W, Niu Z, Zhang H, et al. Imbalance of Th_1/Th_2 and Th_{17}/Treg during the development of uterine cervical cancer. *Int J Clin Exp Pathol.* 2019;12(9):3604-12.[PMID: 31934210 PMCID: PMC6949808]

51. Lin W, Zhang HL, Niu ZY, et al. The disease stage-associated imbalance of Th_1/Th_2 and Th_{17}/Treg in uterine cervical cancer patients and their recovery with the reduction of tumor burden. *BMC Womens Health.* 2020;20(1):126.[PMID: 32552719 PMCID: PMC7301485 DOI: 10.1186/s12905-020-00972-0]

52. Kansy BA, Concha-Benavente F, Srivastava RM,et al. PD-1 Status in $CD8^+$ T Cells Associates with Survival and Anti-PD-1 Therapeutic Outcomes in Head and Neck Cancer. *Cancer Research.* 2017;77(22):6353-64.[PMID: 28904066 PMCID: PMC5690836 DOI: 10.1158/0008-5472.CAN-16-3167]

53. Liu J, Liu D, Hu G, et al. Circulating memory PD-1^+CD8^+ T cells and PD-1^+CD8^+T/PD-1^+CD4^+T cell ratio predict response and outcome to immunotherapy in advanced gastric cancer patients. *Cancer Cell International.* 2023;23(1):274.[PMID: 37974194 PMCID: PMC10655311 DOI: 10.1186/s12935-023-03137-9]

54. Qiu Y, Yang Y, Yang R, et al. Activated T cell-derived exosomal PD-1 attenuates PD-L1-induced immune dysfunction in triple-negative breast cancer. *Oncogene.* 2021;40(31):4992-5001.[PMID: 34172932 PMCID: PMC8342306 DOI: 10.1038/s41388-021-01896-1]

55. Xie F, Xu M, Lu J, Mao L, Wang S. The role of exosomal PD-L1 in tumor progression and immunotherapy. *Molecular Cancer.* 2019;18(1):146.[PMID: 31647023 PMCID: PMC6813045 DOI: 10.1186/s12943-019-1074-3]

56. Kumar S, Chatterjee M, Ghosh P, Ganguly KK, Basu M, Ghosh MK. Targeting PD-1/PD-L1 in cancer immunotherapy: An effective strategy for treatment of triple-negative breast cancer (TNBC) patients. *Genes Dis.* 2023;10(4):1318-50.[PMID: 37397537 PMCID: PMC10311058 DOI: 10.1016/j.gendis.2022.07.024]

57. Hudson K, Cross N, Jordan-Mahy N, Leyland R. The Extrinsic and Intrinsic Roles of PD-L1 and Its Receptor PD-1: Implications for Immunotherapy Treatment. *Front Immunol.* 2020;11:568931.[PMID: 33193345 PMCID: PMC7609400 DOI: 10.3389/fimmu.2020.568931]

58. Xu D, Chen WQ, Liang MX, et al. Tumor-derived small extracellular vesicles promote breast cancer progression by upregulating PD-L1 expression in macrophages. *Cancer Cell Int.* 2023;23(1):137.[PMID: 37452413 PMCID: PMC10347751 DOI: 10.1186/s12935-023-02980-0]

59. Li W, Han G, Li F, et al. Cancer cell-derived exosomal miR-20a-5p inhibits $CD8^+$ T-cell function and confers anti-programmed cell death 1 therapy resistance in triple-negative breast cancer. *Cancer Science.* 2024;115(2):347-56.[PMID: 38129137 PMCID: PMC10859600 DOI: 10.1111/cas.16036]

60. Gholamzadeh Khoei S, Manoochehri H, Saidijam M. Systemic biological study for identification of miR-299-5p target genes in cancer. *Meta Gene.* 2020;24:100655.[https://doi.org/10.1016/j.mgene.2020.100655]

61. Ueda S, Takanashi M, Sudo K, Kanekura K, Kuroda M. miR-27a ameliorates chemoresistance of breast cancer cells by disruption of reactive oxygen species homeostasis and impairment of autophagy. *Lab Invest.* 2020;100(6):863-73.[PMID: 32066826 DOI: 10.1038/s41374-020-0409-4]

62. Li X, Mertens-Talcott SU, Zhang S, Kim K, Ball J, Safe S. MicroRNA-27a Indirectly Regulates Estrogen Receptor {alpha} Expression and Hormone Responsiveness in MCF-7 Breast Cancer Cells. *Endocrinology.* 2010;151(6):2462-73.[PMID: 20382698 PMCID: PMC2875816 DOI: 10.1210/en.2009-1150]